Characterizing wildfire regimes in the United States

Bruce D. Malamud*†, James D. A. Millington*, and George L. W. Perry‡

*Environmental Monitoring and Modelling Research Group, Department of Geography, King's College London, Strand, London WC2R 2LS, United Kingdom; and ‡School of Geography and Environmental Science, University of Auckland, Private Bag 92019, Auckland, New Zealand

Communicated by Donald L. Turcotte, University of California, Davis, CA, February 2, 2005 (received for review August 12, 2004)

Wildfires statistics for the conterminous United States (U.S.) are examined in a spatially and temporally explicit manner. We use a high-resolution data set consisting of 88,916 U.S. Department of Agriculture Forest Service wildfires over the time period 1970–2000 and consider wildfire occurrence as a function of ecoregion (land units classified by climate, vegetation, and topography), ignition source (anthropogenic vs. lightning), and decade. For the conterminous U.S., we (*i*) find that wildfires exhibit robust frequency–area power-law behavior in 18 different ecoregions; (*ii*) use normalized power-law exponents to compare the scaling of wildfire-burned areas between ecoregions, finding a systematic change from east to west; (*iii*) find that wildfires in the eastern third of the U.S. have higher power-law exponents for anthropogenic vs. lightning ignition sources; and (*iv*) calculate recurrence intervals for wildfires of a given burned area or larger for each ecoregion, allowing for the classification of wildfire regimes for probabilistic hazard estimation in the same vein as is now used for earthquakes.

frequency–area statistics | power-law distribution | Bailey ecoregion divisions | U.S. Department of Agriculture Forest Service | probabilistic hazard

Over the last decade, high-profile wildfires (1, 2) have resulted in numerous fatalities and loss of infrastructure. Wildfires also have a significant impact on climate and ecosystems; recently, several researchers (3–7) have emphasized the need for regional-level examinations of wildfire-regime dynamics and change, and the factors driving them. With implications for hazard management, climate studies, and ecosystem research, there is, therefore, significant interest in appropriate analysis of historical wildfire databases. Insightful studies using wildfire database statistics exist (5–24) but are often hampered by the low spatial and/or temporal resolution of their data sets. Here, we use a high-resolution database of wildfires for the conterminous United States (U.S.), combined with techniques drawn from recent advances in statistical physics and complexity theory, to examine U.S. wildfire statistics in a spatially and temporally explicit manner.

Statistical physics and complexity theory have begun to be applied to a wide range of natural hazards (e.g., refs. 25 and 26). One characteristic of many of these studies is power-law (scale-invariant) statistical distributions (27), in which the probability of a certain value occurring is raised to some power of that value. For instance, earthquakes follow a power-law relationship of the frequency (number) vs. energy released, the Gutenberg–Richter relationship (28). The frequency–size statistics of many other natural hazards also appear to satisfy power-law distributions to a good approximation under a wide variety of conditions (29). These natural hazards include asteroid impacts (30, 31), landslides (32, 33), volcanic eruptions (34), and the subject of this paper, wildfires. Power-laws and other "heavy-tailed" distributions are increasingly being used by reinsurance companies and governments for probabilistic hazard analysis (35, 36) and are playing a growing role in environmental and social policy decisions.

The wildfire regime encompasses the timing, frequency, and magnitude of all wildfires that occur in a region. The term "wildfire," as used in this paper, is taken to mean any burned area, irrespective of size or ignition source. Recent studies of wildfire regimes suggest frequency–area probability distributions that are power-law (8–13) or otherwise "heavy-tailed" (14–19) over many orders of wildfire area. The power-law takes the form

$$\dot{f}(A_F) = \alpha A_F^{-\beta}, \quad [1]$$

with frequency density $\dot{f}(A_F)$, the number of wildfires in "unit" bins with A_F burned area, and β and α constants. Local and broad regional studies of wildfires in the U.S. (9), Australia (9), Italy (10), and China (12), for example, have shown power-law behavior with exponents ranging from $\beta = 1.1$–1.8, over two to five orders of magnitude of wildfire area, for 120–9,000 individual wildfire events. However, the low spatial and temporal resolution of the data sets used in these studies has made analyses as a function of wildfire regime drivers difficult. Therefore, in this paper, we use a high-resolution data set (discussed in the next section) consisting of U.S. Department of Agriculture Forest Service (USFS) wildfire-occurrence records [ref. 37; the wildfire data discussed in ref. 37 were obtained through personal communication with T. J. Brown (University of Nevada, Reno)] for $N_{FT} = 88{,}916$ wildfires ($A_F \geq 0.004$ km^2 = 1 acre) between 1970 and 2000. We then examine the resultant wildfire burned-area statistics both spatially and temporally at regional scales as a function of ecological and anthropogenic driving factors. First, we will discuss the data and methods; next, the results of analyses; and, finally, the general implications of having robust power-law behavior for wildfire statistics in each ecoregion.

Data and Methods

Data Quality and Completeness. Using 657,949 wildfires recorded between 1970 and 2000 by the USFS and the U.S. Department of the Interior (DOI), Brown *et al.* (37) compiled an inventory and performed a coarse assessment of the quality of historical federal wildland wildfire-occurrence records. They found 90.7% (324,122 wildfires) of USFS records and 71.0% (214,687 wildfires) of the DOI records "useable" in terms of their completeness and spatial coordinates. Furthermore, they note that DOI wildfire reporting was not continuous for most of the 1970s and that for both the USFS and DOI data, counts of very small wildfire sizes are often incomplete because wildfires may go undetected or unreported. Therefore, in our study we use only those Brown *et al.* (37) records (*i*) from the USFS and (*ii*) with areas $A_F \geq 0.004$ km^2 = 1 acre, giving in our data set (for 1970–2000) a total number of wildfires $N_{FT} = 88{,}916$ and total area burned $A_{FT} = 68{,}994$ km^2 (see Table 1 for numbers of wildfires and area burned per ecoregion). Wildfires in our study were classified as "anthropogenic" (64% by number) or "lightning" (36%) according to the description given by Brown *et al.* (37). All nonanthropogenic fires are here termed "lightning," because of the very small occurrence (<0.01%) of "other" natural causes (e.g., volcanism) (37).

Abbreviations: U.S., United States; USFS, U.S. Department of Agriculture Forest Service.

†To whom correspondence should be addressed. E-mail: bruce@malamud.com.

www.pnas.org/cgi/doi/10.1073/pnas.0500880102

Table 1. Results by Bailey ecoregion divisions in the conterminous U.S. for frequency–area and recurrence-interval analyses of USFS wildfires

Ecoregion division name	Ecoregion division code	Ecoregion division area, km²	USFS area, km²	A_{FT}, km²	N_{FT}	β	logα	r^2	T (≥0.01 km²), yr	T (≥10 km²), yr
Hot Continental	[220]	969,955	32,068	1,132.4	8,429	1.75 ± 0.11	−3.81 ± 0.12	0.974	0.19 ± 0.10	34 ± 20
Hot Continental Mtns.	[M220]	192,955	43,609	815.4	7,353	1.75 ± 0.09	−4.05 ± 0.10	0.984	0.30 ± 0.14	55 ± 27
Marine	[240]	38,591	1,147	8.0	58	1.37 ± 0.21	−3.99 ± 0.31	0.972	0.89 ± 0.69	23 ± 22
Marine Mtns.	[M240]	138,300	67,360	2,813.5	3,875	1.53 ± 0.05	−4.36 ± 0.07	0.989	2.47 ± 0.73	100 ± 37
Mediterranean	[260]	88,319	2,546	2,918.6	475	1.30 ± 0.05	−3.44 ± 0.07	0.987	0.22 ± 0.05	2 ± 1
Mediterranean Mtns.	[M260]	241,388	99,798	16,055.4	11,882	1.46 ± 0.05	−3.93 ± 0.06	0.989	0.51 ± 0.13	13 ± 4
Prairie	[250]	772,597	1,583	39.4	316	1.48 ± 0.15	−3.60 ± 0.19	0.964	0.28 ± 0.19	9 ± 8
Savanna	[410]	20,202	0	0	0					
Subtropical	[230]	1,064,749	42,920	2,670.2	16,423	1.81 ± 0.07	−3.74 ± 0.09	0.987	0.12 ± 0.05	33 ± 14
Subtropical Mtns.	[M230]	22,792	6,667	142.0	1,816	1.70 ± 0.12	−3.82 ± 0.15	0.974	0.24 ± 0.15	32 ± 21
Temperate Desert	[340]	689,458	39,210	3,890.7	2,391	1.39 ± 0.05	−4.09 ± 0.07	0.985	0.85 ± 0.22	13 ± 5
Temperate Desert Mtns.	[M340]	112,924	27,289	1,027.9	885	1.39 ± 0.07	−4.38 ± 0.08	0.984	1.66 ± 0.54	27 ± 13
Temperate Steppe	[330]	1,099,973	43,841	3,034.5	2,466	1.46 ± 0.05	−4.18 ± 0.06	0.990	0.89 ± 0.23	22 ± 8
Temperate Steppe Mtns.	[M330]	585,081	300,383	26,281.0	15,487	1.49 ± 0.04	−4.34 ± 0.06	0.993	1.18 ± 0.26	36 ± 10
Tropical/Subtropical Desert	[320]	447,811	13,306	1,658.4	2,379	1.47 ± 0.07	−3.69 ± 0.08	0.984	0.29 ± 0.09	8 ± 3
Tropical/Subtropical Steppe	[310]	657,342	28,536	2,179.6	4,138	1.57 ± 0.06	−3.95 ± 0.07	0.990	0.40 ± 0.12	20 ± 7
Tropical/Subtropical Steppe Mtns.	[M310]	130,018	42,861	3,949.3	8,594	1.54 ± 0.06	−3.93 ± 0.07	0.989	0.41 ± 0.12	18 ± 6
Warm Continental	[210]	381,507	47,453	374.4	1,888	1.69 ± 0.08	−4.71 ± 0.10	0.988	1.70 ± 0.76	203 ± 99
Warm Continental Mtns.	[M210]	112,924	5,983	2.9	61	1.68 ± 0.28	−5.18 ± 0.41	0.988	13.64 ± 12.88	1,672 ± 1616
Totals		7,766,886	846,560	68,993.6	88,916					

Given for each Bailey ecoregion division (38) (Fig. 1*A*) in the conterminous U.S. are the following: division name; division code (M = mountain areas); area of division; area of USFS lands within the ecoregion division (Fig. 1*B*); the total area, A_{FT}, and total number, N_{FT} of wildfires occurring in USFS lands (1970–2000) irrespective of ignition source and included in the data set used for analyses in this paper (ref. 37; and see *Data and Methods*); and the results of frequency–area and recurrence-interval analyses. Frequency–area parameters β and logα are from Eq. **1**, $\dot{f}(A_F) = \alpha A_F^{-\beta}$, where in each case the best fit was estimated for $\log[\dot{f}(A_F)] = -\beta \log[A_F] + \log\alpha$, with coefficient of determination r^2 as given. Error bars on β and logα are $\pm 2\sigma$ (standard deviations) and approximately equivalent to upper/lower 95% confidence intervals. Error bars were obtained from each variable's standard error and degrees of freedom based on the number of 'bins' used in the least-squares fit. For completeness, all fits are shown; however, care should be taken in interpreting β and logα based on small data samples (e.g., $N_{FT} <$ 100). Recurrence intervals $T(\geq A_F)$ are obtained from Eq. **5** and represent the average time between wildfires ≥0.01 km² and ≥10 km², occurring in spatial areas of 1,000 km² within each ecoregion. Associated error bars again represent $\pm 2\sigma$ (standard deviations) or 95% confidence intervals, calculated for each ecoregion by using the upper/lower 95% confidence interval values as given in this table for β and logα.

Bailey's Ecoregions. To allow spatial analyses with regard to the biophysical factors that drive wildfire regimes, we classify the USFS wildfire data into the ecoregion divisions developed by Bailey (38) (Fig. 1*A*). Ecoregions distinguish geographic regions that share common biophysical characteristics. In Bailey's classification (38), a three-level hierarchy is used: domains (based primarily on climate), divisions (climate, vegetation, and soils), and provinces (climate, vegetation, soils, land-surface form, and fauna). Mountainous areas within specific divisions and provinces are also classified. In the conterminous U.S., there are three domains, subdivided into 19 divisions and further divided into 34 provinces. Ecoregion divisions are shown in Fig. 1*A*, with division names, codes, and areas in Table 1. Using Bailey's ecoregion division level in our analyses allows spatial disaggregation of the data, at a resolution suitable for the study of potential wildfire-regime drivers, while ensuring that an adequate number of wildfires are available for statistical analyses. Wildfires occurring on USFS lands are used as a representative sample of the ecoregion division in which they are located. USFS land area per ecoregion is given in Table 1, with the spatial distribution in the conterminous U.S. shown in Fig. 1*B*. Of the 18 ecoregion divisions with wildfire data, USFS lands range from 0.2% (Prairie) to 51.3% (Temperate Steppe Mtns.) of the respective ecoregion's area.

Frequency–Area Statistics. In each ecoregion division, we examine the frequency–area statistics of USFS wildfires. Because the wildfire inventories used are not "complete" (there are many more "smaller" wildfires than measured), probability densities are not appropriate; instead, we use frequency densities $f(A_F)$ defined as

$$f(A_F) = \frac{\delta N_F}{\delta A_F}, \qquad [2]$$

where A_F is the wildfire burned area and δN_F is the number of wildfires in a "bin" of width δA_F. The frequency densities $f(A_F)$ are then the number of wildfires per "unit" bin. We use frequency densities because cumulative frequencies can obscure underlying trends in finite data sets (39). Because there are many more small wildfires than larger ones, we increase our bin width δA_F with increasing area A_F, to give approximately equal bin widths in logarithmic coordinates. The USFS areas over which the wildfires occur change from one ecoregion to another (Table 1 and Fig. 1*B*). Therefore, to allow specific comparison between ecoregions, we take the frequency densities $\dot{f}(A_F)$ (fires·km^{-2}) and normalize them by (*i*) the USFS area (km²) within each ecoregion and (*ii*) the period of observation (yr), to give normalized frequency densities $\dot{f}(A_F)$ (fires·yr^{-1}·km^{-4}).

For each ecoregion division, the normalized frequency densities $\dot{f}(A_F)$ are plotted as a function of wildfire area A_F. As we will show later (see *Results*), an excellent fit in each case is given by the inverse power-law distribution (Eq. **1**), a two-parameter distribution that forms a straight line in log–log space. In each case, we estimate the best fit for $\log[\dot{f}(A_F)] = -\beta \log[A_F] + \log\alpha$, where β is the gradient and logα is the y-intercept. The power-law exponent β quantifies the ratio of the number of large to small wildfires in a given area, with $\beta = 0$ indicating the same number of large as small wildfires (per "unit" size bins). As β increases, large events become rarer with respect to small ones. The y-intercept, or logα, is the normalized number of wildfires per unit bin; in our case, $A_F = 1$ km².

Calculation of Recurrence Intervals. An extension of having the two parameters α and β in the inverse power-law distribution given

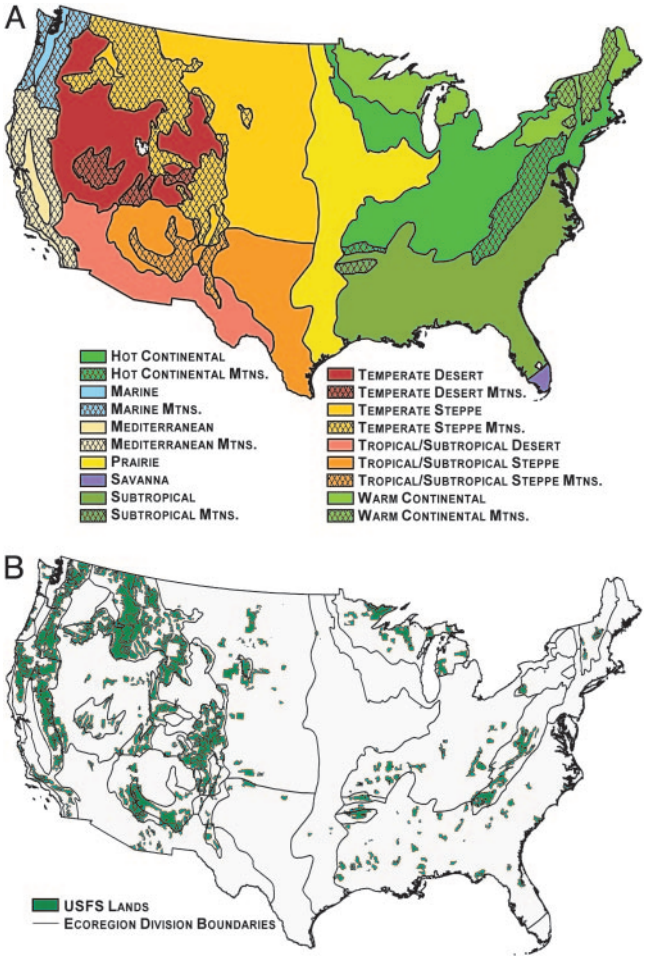

Fig. 1. Bailey's ecoregion divisions and USFS lands. (*A*) In Bailey's classification (38), the conterminous U.S. is divided into ecoregion divisions according to common characteristics of climate, vegetation, and soils. Mountainous areas within specific divisions are also classified. In this paper, we use ecoregion divisions to geographically subdivide an extensive database of wildfire-burned areas for statistical analyses as a function of ecoregion division. (*B*) Location of USFS lands in the conterminous U.S. Table 1 gives each ecoregion division area and the total area of USFS lands within each ecoregion.

in Eq. **1** is the calculation of the recurrence interval $T(\geq A_F)$, based on the probability that in a defined spatial area (i.e., some specific region A_R), a given size event with area A_F will be equaled or exceeded in any given year. For example, if in a defined region there is an average 1 in 100 chance per year that a wildfire of area ≥ 10 km^2 will occur, this size event (10 km^2) is said to have a 100-yr recurrence interval. In other words, assuming that the events are uncorrelated in time (Poissonian), then for this region there will be, on average, 100 yr between wildfires of size 10 km^2 or greater. In calculating the recurrence intervals associated with different wildfire areas A_F, we first take the integral of Eq. **1** to arrive at $N_{CF}(\geq A_F)$, the cumulative number of wildfires with areas greater than or equal to A_F, giving (for $\beta > 1$)

$$N_{CF}(\geq A_F) = \int_{A_F}^{\infty} f(A'_F)\,dA'_F = \tau A_R \left(\frac{\alpha}{\beta - 1}\right) A_F^{1-\beta}, \qquad [3]$$

where α and β are constants from Eq. **1**, τ is the data set duration in years, and A_R is the spatial area over which the probabilistic "hazard" is to be considered. As A_R increases, the number of wildfires of a given size or larger $N_{CF}(\geq A_F)$ in that region also increases. We could terminate the integral in Eq. **3** at some A_{max} instead of infinity, because the power-law distribution given in Eq. **1** must have some upper bound. However, because the numbers of the most extreme events are few, the shape of the tail at these extreme values is unclear. Therefore, we choose to consider "small" and "medium" values of A_F, well below the maximum wildfire area that might occur in any given ecoregion.

Using a Weibull equation, the recurrence interval $T(\geq A_F)$ associated with a wildfire of a given area or larger is $\tau + 1$, the total number of years in the data set plus one, divided by $N_{CF}(\geq A_F)$, giving (for $\beta > 1$)

$$T(\geq A_F) = \frac{\tau + 1}{N_{CF}(\geq A_F)} = \left(\frac{\tau + 1}{\tau}\right)\left(\frac{\beta - 1}{\alpha}\right)\left(\frac{A_F^{\beta-1}}{A_R}\right). \qquad [4]$$

The length of our data set is $\tau = 31$ yr, and we consider the recurrence interval of wildfires in spatial areas of $A_R = 1{,}000$ km^2, giving (for $\beta > 1$)

$$T(\geq A_F) = 1.032 \times 10^{-3}\ \text{km}^2 \left(\frac{\beta - 1}{\alpha}\right) A_F^{\beta-1}, \qquad [5]$$

with A_F in km^2 and $T(\geq A_F)$ in years. In *Results*, we present recurrence intervals by ecoregion for $A_F = 0.01$ km^2 and $A_F = 10$ km^2 for spatial areas within each ecoregion of $A_R = 1{,}000$ km^2.

Results

Frequency–Area Statistics of Wildfires. In Table 1, for each ecoregion division, we give the results of our normalized frequency–area analyses. Each ecoregion division exhibits excellent frequency–area power-law behavior ($r^2 \geq 0.96$) over more than five orders of magnitude for burned area. In each case, the wildfire statistics have been examined as a function of ecoregion division, regardless of ignition source (lightning vs. anthropogenic). Also included in Table 1 are $\pm 2\sigma$ error bars (see legend) equivalent to lower/upper 95% confidence intervals for both β and logα. Two example analyses are given in Fig. 2, with the Mediterranean Ecoregion ($\beta = 1.30 \pm 0.05$) and the Subtropical Ecoregion ($\beta = 1.81 \pm 0.07$) exhibiting the smallest and largest β values for the 18 ecoregions, respectively. Note that care should be taken in interpreting parameter values for ecoregion divisions with very small wildfire numbers (e.g., $N_{FT} < 100$; Marine and Warm Continental Mtns.), because these have increased uncertainty in estimates for β and logα.

Spatial Distribution of β. We next map the spatial distribution of β values by ecoregion (Fig. 3*A*), where β is the result of each frequency–area analysis shown in Table 1. Fig. 3*A* suggests an east-to-west gradient of higher-to-lower β values across the conterminous U.S. We note that Fig. 3*A* does not take into account the $\pm 2\sigma$ error bars on β (95% confidence intervals) as given in Table 1. However, even taking the error bars into account, there is still strong evidence of the east-to-west gradient of β values across the conterminous U.S.

Lightning vs. Anthropogenic Wildfires. To explore alternative hypotheses given for the east-to-west gradient of β, we examine wildfire records with reference to ignition source, whether natural (lightning) or anthropogenic. The numbers of anthropogenic vs. lightning wildfires in our data set varies as a function of ecoregion division, with the ratio ($N_{F\ \text{anthropogenic}}/N_{F\ \text{lightning}}$) = 0.2–0.8 in the seven Temperate and Tropical/Subtropical ecoregions (all divisions with codes >300); 1.2–4.7 in Marine, Marine Mtns., Mediterranean Mtns., and Subtropical Mtns.; and 11–43 in the remaining seven ecoregion divisions.

Within each ecoregion division, we examine $\beta_{anthropogenic}$ and

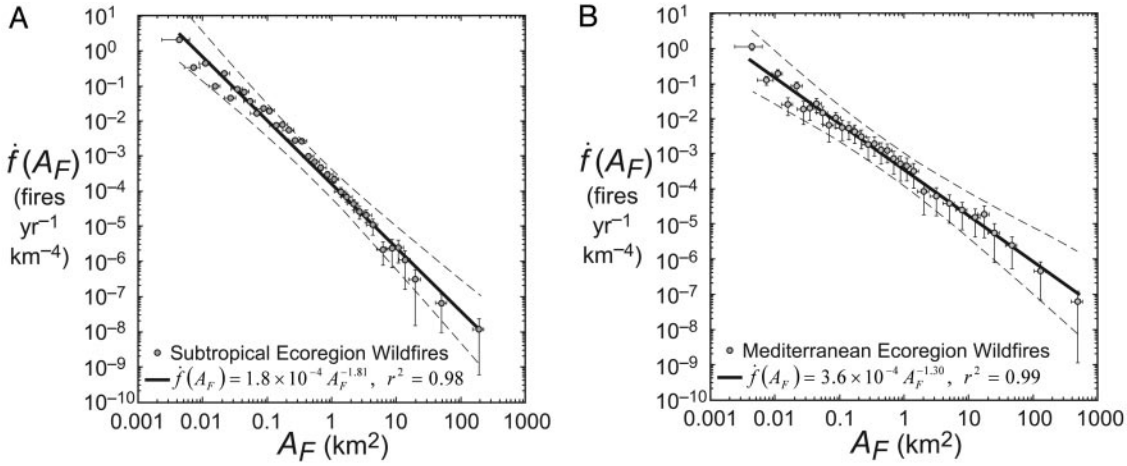

Fig. 2. Normalized frequency–area wildfire statistics for Subtropical (*A*) and Mediterranean (*B*) ecoregions (1970–2000; data from ref. 37). Shown (circles) are normalized frequency densities $\dot{f}(A_F)$ (number of wildfires per ''unit bin'' of 1 km^2, normalized by database length in years and USFS area within the ecoregion) plotted as a function of wildfire area A_F. Also shown for both ecoregions is a solid line, the best least-squares fit to $\log[\dot{f}(A_F)] = -\beta \log[A_F] + \log\alpha$, with coefficient of determination r^2. Dashed lines represent lower/upper 95% confidence intervals, calculated from the standard error. Horizontal error bars on burned area A_F are due to measurement and size binning of individual wildfires (A_F from 1–5 acres has primary peaks in wildfire occurrence at integer values; 5–30 acres, every 5 acres; 30–100 acres, every 10 acres; etc.). Therefore, for $A_F = 0.0040–0.010$ km^2 (1.0–2.5 acres), we use 0.5-acre horizontal error bars of ± 0.0020 km^2, and for $A_F \geq 0.010$ km^2, horizontal error bars of $\pm 0.2 A_F$. Vertical error bars represent two standard deviations ($\pm 2\sigma$) of the normalized frequency densities $\dot{f}(A_F)$, calculated as $\pm 2\sqrt{\delta N_F}$ (normalized by database length in years and USFS area within the ecoregion), where δN_F is the number of wildfires in a ''bin'' of width δA_F. The $\pm 2\sigma$ error bars are approximately the same as the lower and upper 95% confidence interval ($\pm 1.96\sigma$). Table 1 summarizes the results for all ecoregion divisions.

$\beta_{\text{lightning}}$ and find $(\beta_{\text{anthropogenic}}/\beta_{\text{lightning}}) > 1$ in the eastern third of the U.S. (35% by area), where $\beta_{\text{anthropogenic}}/\beta_{\text{lightning}} = 1.30$ (Hot Continental), 1.21 (Warm Continental), 1.14 (Hot Continental Mtns.), and 1.12 (Subtropical). Most other areas have $(\beta_{\text{anthropogenic}}/\beta_{\text{lightning}}) \approx 1$ (within $\pm 2\sigma$ error bars, as described in Table 1 legend), except for the Temperate Steppe division, where $(\beta_{\text{anthropogenic}}/\beta_{\text{lightning}}) = 0.88$. At Bailey's ecoregion ''domain'' level (38), where divisions with related climates are grouped, we find that ecoregion divisions with $(\beta_{\text{anthropogenic}}/\beta_{\text{lightning}}) > 1$ generally fall into the Humid Temperate domain.

Wildfire Statistics as a Function of Decade. In each ecoregion we also examine the wildfire data by decade (1970–1979, 1980–1989, and 1990–1999), both by different ignition source and for all fires irrespective of ignition source. We find similar results for β and $\log\alpha$ as for the entire 31-yr period (Table 1). However, there is a small (statistically nonsignificant) decrease of 3–12% in β values from the decades 1970s to 1990s for all ecoregions except Warm Continental Mtns., Marine, and Prairie (each of which have scant data).

Wildfire Recurrence Intervals. For each ecoregion we use Eq. **5** to calculate recurrence intervals $T(\geq 0.01$ km$^2)$ and $T(\geq 10$ km$^2)$. This probabilistic hazard analysis gives us the average time between events with burned areas greater than or equal to 0.01 and 10 km^2, respectively, occurring in a defined spatial ''area'' within each ecoregion. For comparison between ecoregions, we will consider relatively small spatial areas of size 1,000 km^2.

To examine the strength of temporal correlation in wildfire areas (also see ref. 24), we examined the time lags between successive wildfire areas for specific ecoregion divisions, taking different lower cutoff bounds for the wildfire areas used. We find that the wildfire events exhibit short-term but not long-term memory; the smallest wildfire areas are correlated in time, but the medium and large ones are approximately uncorrelated (i.e., Poissonian). For medium and large events, this allows us to calculate recurrence intervals based on the results of the frequency–area wildfire statistics found earlier in Table 1.

Using Eq. **5**, the recurrence intervals $T(\geq A_F)$ for each ecoregion division are given in Table 1, including $\pm 2\sigma$ error bars as calculated from the error bars on β and $\log\alpha$. Because of the small amount of data used to fit the medium/upper tail of the distribution in Eq. **1**, the $\pm 2\sigma$ error bars on $T(\geq A_F)$ are large, averaging 30–60% of the actual recurrence interval value. Despite this, there are clear differences between ecoregions. For example, the Mediterranean Ecoregion has $T(\geq 10$ km$^2) = 2 \pm 1$ yr. In other words, for any 1,000-km^2 ''area'' in this ecoregion, we ''expect'' on average one wildfire with burned area $A_F \geq 10$ km^2 every 1–3 yr (33–100% probability of occurring in any year). By contrast (Table 1), the Warm Continental Ecoregion has $T(\geq 10$ km$^2) = 203 \pm 99$ yr; the occurrence probability for a wildfire with $A_F \geq 10$ km^2 has dropped significantly to 0.3–1.0% in any given year, a factor of $\approx$100 between the two ecoregion divisions. A spatial mapping for $T(\geq 10$ km$^2)$ is given in Fig. 3*B*. For both the eastern and western thirds of the U.S., there is a gradient from large to small recurrence intervals (i.e., lower to higher hazard) going from north to south, with the largest recurrence intervals of wildfires (lowest hazard) in the northeast U.S. Our method for calculating wildfire-recurrence intervals gives a simple and quick way of determining approximate quantitative hazard assessments of given size wildfires (or larger) occurring across the conterminous U.S.

Discussion

Spatial Distribution of β. The east-to-west gradient in β values (Fig. 3*A*) observed at Bailey's ecoregion division level suggests that the ratio of the number of large to small wildfires decreases from east to west across the conterminous U.S. Controls on the wildfire regime (e.g., climate and fuels) vary temporally, spatially, and at different scales (3), so it is difficult to attribute specific causes to this east-to-west gradient. For example, the observed reduced contribution of large wildfires to total burned area (i.e., β large) in eastern ecoregion divisions may be due to greater human population densities that increase forest fragmentation compared with western ecoregions (40). Alternatively, the observed gradient may have natural drivers, with

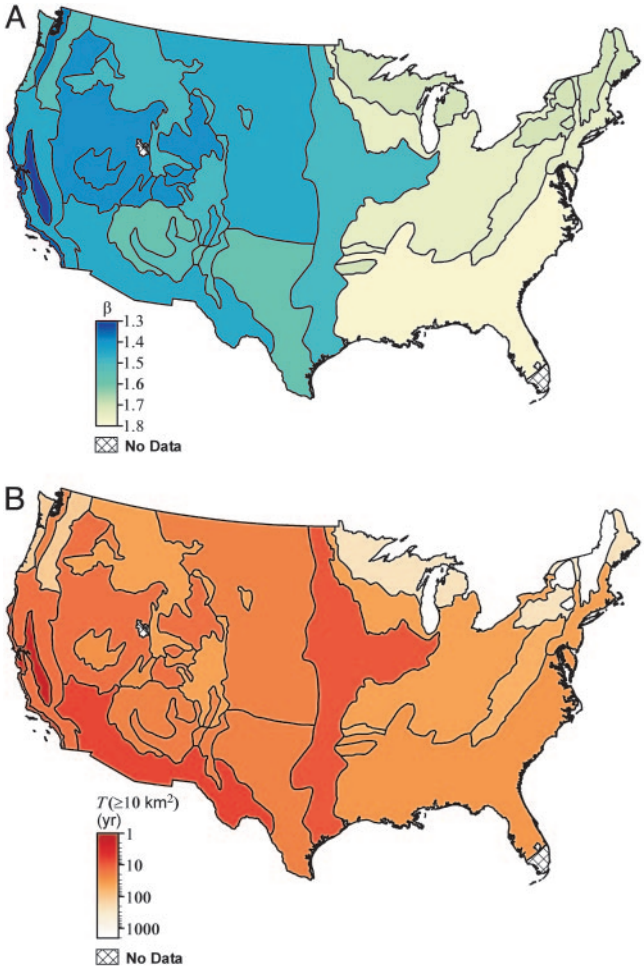

Fig. 3. Spatial mapping of β and recurrence interval T by ecoregion division. Shown across the conterminous U.S. for 1970–2000 are the results of frequency–area statistics (Table 1) for USFS wildfires classified by ecoregion division (Fig. 1). (*A*) Spatial distribution of β (power-law exponent in Eq. **1**), representing the ratio of how many large vs. small wildfire areas occur in each ecoregion division. (*B*) Recurrence intervals $T(\geq A_F)$ (Eq. **5**) for $A_F = 10$ km^2, or how many years on average a wildfire 10 km^2 or larger would be expected in spatial areas of 1,000 km^2 within each ecoregion division. The legend colors go from dark red (small recurrence intervals) to white (large recurrence intervals), representing ''high'' to ''low'' hazard, with the legend scale in years increasing logarithmically. For *A* and *B*, $\pm 2\sigma$ error bars for β and $T(\geq A_F)$ are given in Table 1.

climate and vegetation producing conditions more conducive to large wildfires in some ecoregions compared with others.

In other studies, gradients similar to that observed here have been described and related to climate and vegetation. Turner *et al.* (41) describe wildfire-occurrence gradients, as a function of altitude and latitude, in crown fire ecosystems in continental northern North America. They attribute these gradients to broad climatic variations and note that western and central regions tend to have relatively frequent fires with forest stand structures dominated by younger individuals, whereas the eastern region experiences longer inter-fire intervals and older stand structures. Other studies (5, 22, 23, 42) have found climatic variability to be a dominant factor affecting wildfire regimes at large temporal and spatial resolutions and extents. A broad-scale gradient in wildfire-regime characteristics across potential natural vegetation types has also been observed in the U.S. (42) and Spain (6). Potential natural vegetation is the successional endpoint (''climax'') vegetation of an area, in the absence of climate change or human disturbance.

To examine potential drivers of the east-to-west gradient in β values observed, we also examined wildfire records with reference to ignition source. The ratio $\beta_{\text{anthropogenic}}/\beta_{\text{lightning}} > 1$ in the eastern third of the conterminous U.S. suggests a potential influence of human activity on the relative scaling of wildfire-burned areas, because these areas are more populated. It has been suggested (20) that increased landscape heterogeneity decreases disturbance (e.g., wildfire) spread. Historic anthropogenic forest clearance, resulting in forests fragmented by agricultural and urban land cover, has increased the heterogeneity of eastern landscapes (40). This may have reduced the relative number of large to small fires in the east compared to the west. In western landscapes, forests have also become fragmented, but via replacement by shrublands and grasslands (40) that are more conducive to wildfire spread than the agricultural and urban land covers that have fragmented eastern forests.

We suggest that the use of the power-law exponent β to characterize wildfire regimes, in a similar fashion used in this paper, will be useful in future wildfire-regime studies. In our analyses, the influence of climatic factors on the observed east-to-west gradient in β across the conterminous U.S. is not clear. However, examining the relationships between β and past/current climates could aid estimates of future wildfire regime behavior (specifically the scaling of fire sizes) by linking these relationships to models of future climate change. Furthermore, research considering the spatial relationship between β and net primary production (the total stored energy/biomass produced by photosynthesis, minus the energy used in autotrophic respiration, in a unit area) may be useful in examining human impacts on the relative scaling of wildfire-burned areas due to management or manipulation of vegetated lands.

Self-Organization in Wildfire Regimes. Wildfires influence vegetation, which, in turn, influences future wildfire activity (43). Within ecosystems, the feedbacks between process (the wildfires) and the ecological patterns (vegetation type, age, physiognomy, etc.) produce both spatial complexity and temporal memory effects (44, 45). Both spatially and temporally, a ''structured'' pattern results, with some degree of spatial and temporal autocorrelation. The patterns in vegetation both constrain, and are in turn constrained by, the processes that generate them. For an area of forest that has never been burned, after a wildfire occurs there will be a pattern, the ''mosaic,'' of burned and unburned patches of vegetation (e.g., ref. 46). These patterns influence the next wildfire that occurs. Recently burned areas may be less flammable (for example) than older ones. The next wildfire is constrained by the old pattern but will create a new one, and the feedback continues (47).

In this article, we have discussed power-law or scale-invariant statistical distributions for wildfire-burned areas. Bolliger *et al.* (48) queried whether, in nature, self-organizing dynamics would overcome environmental gradients to ensure power-law behavior. We certainly acknowledge that there are always upper and lower cut-offs in nature for any power-law behavior, and the same is true for wildfires. For instance, in the case of wildfires, an upper boundary might be the barrier presented by a mountain range or high topography dividing drainage networks. A lower boundary might be the partial burning of a single tree or bush, or fine-scale discontinuities in the fuel bed. However, despite these feedbacks and upper/lower boundaries, we have shown that wildfires within each of 18 different ecoregion divisions have frequency–area relationships that are robustly scale-invariant over more than five orders of burned area.

This robust power-law (scale-invariant) behavior of wildfire areas might be taken as evidence that ecosystems self-organize through the feedbacks described above to ensure that energy is dissipated at the maximum rate across all scales. Self-organization has previously been discussed for both real and

model ecosystems (9–12, 25, 47, 49–53). Thus, variation in β between ecoregions may indicate differences in energy balance and rates of energy release in ecosystems according to differences in climate. An examination of β and its spatial and temporal relationships with the net primary production and the potential natural vegetation, in conjunction with more accurate estimates of energy released during combustion currently being developed (54), would contribute to understanding the role of wildfire in ecosystem energetics and the organization within open, dissipative systems (such as ecosystems) in general.

Recurrence Intervals of Wildfires. Using both α and β, we have calculated the recurrence intervals $T(\geq 0.01\ \text{km}^2)$ and $T(\geq 10\ \text{km}^2)$ for each ecoregion division (Table 1 and Fig. 3*B*). This type of mapping, and extensions of it, will prove very useful for government agencies and reinsurance groups when examining wildfire hazard.

Conclusions

Wildfires are costly in terms of damage and fatalities. The ways in which they begin and propagate are complex, with an individual wildfire depending strongly on meteorological conditions, topography, vegetation, and, of course, wildfire-fighting efforts. Despite this complexity, the frequency–area of wildfires in conterminous U.S. ecoregions appear to robustly follow power-law (heavy-tailed) distributions, over more than five orders of burned area in each ecoregion. The simplicity of accepting power-law (or similar heavy-tailed) distributions, which exhibit scale-invariant behavior with excellent fits over many orders of magnitude, allows the use of the parameters β and α to describe the relative contribution and hazard of large wildfires within a wildfire regime. In turn, normalized β and α values allow for the explicit comparison and examination of wildfire-regime dynamics and change between ecoregions, as illustrated here.

We thank Timothy J. Brown, for access to the USFS wildfire data set. We also thank the two reviewers, Ian Main (University of Edinburgh) and Malcolm Gill (Centre for Plant Biodiversity Research, Canberra, Australia), for their constructive and comprehensive comments. The contributions of B.D.M. were partially supported by United Kingdom Natural Environment Research Council/Engineering and Physical Sciences Research Council Grant NER/T/S/2003/00128.

1. Reichhardt, T. (2002) *Nature* **418,** 3–4.
2. Food and Agriculture Organization of the United Nations (2001) *Global Forest Fire Assessment 1990–2000*, Forest Resources Assessment Programme Working Papers (Food and Agriculture Organization of the United Nations, Rome), No. 55.
3. Schoennagel, T., Veblen, T. T. & Romme, W. H. (2004) *BioScience* **54,** 661–676.
4. Cleland, D. T., Crow, T. R., Saunders, S. C., Dickmann, D. I., Maclean, A. L., Jordan, J. K., Watson, R. L., Sloan, A. M. & Brosofske, K. (2004) *Landscape Ecol.* **19,** 311–325.
5. Grissino-Mayer, H. D. & Swetnam, T. W. (2000) *Holocene* **10,** 213–220.
6. Vazquez, A., Perez, B., Fernandez-Gonzalez, F. & Moreno, J. M. (2002) *J. Veg. Sci.* **13,** 663–676.
7. Morgan, P., Hardy, C. A., Swetnam, T. W., Rollins, M. G. & Long, D. G. (2001) *Int. J. Wildland Fire* **10,** 329–342.
8. Minnich, R. A. (1983) *Science* **219,** 1287–1294.
9. Malamud, B. D., Morein, G. & Turcotte, D. L. (1998) *Science* **281,** 1840–1842.
10. Ricotta, C., Avena, G. & Marchetti, M. (1999) *Ecol. Modell.* **119,** 73–77.
11. Ricotta, C., Arianoutsou, M., Díaz-Delgado, R., Duguy, B., Lloret, F., Maroudi, E., Mazzoleni, S., Moreno, J. M., Rambal, S., Vallejo, R., *et al.* (2001) *Ecol. Modell.* **141,** 307–311.
12. Song, W. G., Fan, W. C., Wang, B. H. & Zhou, J. J. (2001) *Ecol. Modell.* **145,** 61–68.
13. McCarthy, M. A. & Gill, A. M. (1997) in *Frontiers in Ecology*, eds. Klomp, N. & Lunt, I. (Elsevier, Oxford), pp. 79–88.
14. Li, C., Corns, I. G. W. & Chang, R. C. (1999) *Landscape Ecol.* **14,** 533–542.
15. Cumming, S. G. (2001) *Can. J. For. Res.* **31,** 1297–1303.
16. Minnich, R. A. & Chou, Y. H. (1997) *Int. J. Wildland Fire* **7,** 221–248.
17. Reed, W. J. & McKelvey, K. S. (2002) *Ecol. Modell.* **150,** 239–254.
18. Ricotta, C. (2003) *Comments Theor. Biol.* **8,** 93–101.
19. Schoenberg, F. P., Peng, R. & Woods, J. (2003) *Environmetrics* **14,** 583–592.
20. Lloret, F., Calvo, E., Pons, X. & Díaz-Delgado, R. (2002) *Landscape Ecol.* **17,** 745–75.
21. Vazquez, A. & Moreno, J. M. (1998) *Int. J. Wildland Fire* **8,** 103–115.
22. Pierce, J. L., Meyer, G. A. & Jull, A. J. T. (2004) *Nature* **432,** 87–90.
23. Weisberg, P. J. & Swanson, F. J. (2003) *For. Ecol. Manage.* **172,** 17–28.
24. Díaz-Delgado, R., Lloret, F. & Pons, X. (2004) *Intl. J. Wildland Fire* **13,** 89–99.
25. Turcotte, D. L., Malamud, B. D., Guzzetti, F. & Reichenbach, P. (2002) *Proc. Natl. Acad. Sci. USA* **99,** 2530–2537.
26. Sornette, D. (2004) *Critical Phenomena in Natural Sciences* (Springer, Berlin), 2nd Ed.
27. Hergarten, S. (2004) *Nat. Hazards Earth Syst. Sci.* **4,** 309–313.
28. Gutenberg, B. & Richter, C. F. (1954) *Seismicity of the Earth and Associated Phenomena* (Princeton Univ. Press, Princeton), 2nd Ed.
29. Malamud, B. D. (2004) *Phys. World* **17,** 31–35.
30. Chapman, C. R. & Morrison, D. (1994) *Nature* **367,** 33–40.
31. Chapman, C. R. (2004) *Earth Planet. Sci. Lett.* **222,** 1–15.
32. Guzzetti, F., Malamud, B. D., Turcotte, D. L. & Reichenbach, P. (2002) *Earth Planet. Sci. Lett.* **195,** 169–183.
33. Malamud, B. D., Turcotte, D. L., Guzzetti, F. & Reichenbach, P. (2004) *Earth Surf. Processes Landforms* **29,** 687–711.
34. Pyle, D. M. (2000) in *Encyclopedia of Volcanoes*, eds. Sigurdsson, H., Houghton, B., Rymer, H., Stix, J. & McNutt, S. (Academic, San Diego), pp. 263–269.
35. Embrechts, P., Klüppelberg, C. & Mikosch, T. (1999) *Modelling Extremal Events for Insurance and Finance* (Springer, New York), 2nd Ed.
36. Beirlant, J., Matthys, G. & Dierckx, G. (2001) *ASTIN Bull.* **31,** 37–58.
37. Brown, T. J., Hall, B. L., Mohrle, C. R. & Reinbold, H. J. (2002) *Coarse Assessment of Federal Wildland Fire Occurrence Data*, CEFA Rep. 02-04; www.cefa.dri.edu/Publications.
38. Bailey, R. G. (1995) *Ecosystem Geography* (Springer, New York).
39. Main, I. (2000) *Bull. Seismol. Soc. Am.* **90,** 86–97.
40. Riitters, K. H., Wickham, J. D., O'Neill, R. V., Jones, K. B., Smith, E. R., Coulston, J. W., Wade, T. G. & Smith, J. H. (2002) *Ecosystems* **5,** 815–822.
41. Turner, M. G. & Romme, W. H. (1994) *Landscape Ecol.* **9,** 59–77.
42. McKenzie, D., Gedalof, Z., Peterson, D. L. & Mote, P. (2004) *Conserv. Biol.* **18,** 890–902.
43. Turner, M. G. (1989) *Annu. Rev. Ecol. Syst.* **20,** 171–197.
44. Peterson, G. T. (2002) *Ecosystems* **5,** 329–338.
45. Perry, G. L. W. (2002) *Prog. Phys. Geogr.* **26,** 339–359.
46. Gill, A. M., Allan, G. & Yates, C. (2003) *Int. J. Wildland Fire* **12,** 323–331.
47. Holling, C. S., Peterson, G., Marples, P., Sendzimir, J., Redford, K., Gunderson, L. & Lambert, D. (1996) in *Global Change and Terrestrial Ecosystems*, eds. Walker, B. & Steffen, W. (Cambridge Univ. Press, Cambridge, U.K.), pp. 346–384.
48. Bolliger, J., Sprott, J. C. & Mladenoff, D. J. (2003) *Oikos* **100,** 541–553.
49. Drossel, B. & Schwabl, F. (1992) *Phys. Rev. Lett.* **69,** 1629–1632.
50. Odum, H. T. (1988) *Science* **242,** 1132–1139.
51. Holling, C. S. (1992) *Ecol. Monogr.* **62,** 447–502.
52. Grassberger, P. (2002) *New J. Phys.* **4,** 17.1–17.15.
53. Caldarelli, G., Frondoni, R., Gabrielli, A., Montuori, M., Retzlaff, R. & Ricotta, C. (2001) *Europhys. Lett.* **56,** 510–516.
54. Wooster, M. J., Zhukovb, B. & Oertelb, D. (2003) *Remote Sens. Environ.* **86,** 83–107.